



Universiteit
Leiden
The Netherlands

Electrocatalytic CO₂ reduction toward liquid fuels : on heterogeneous electrocatalysts and heterogenized molecular catalysts

Birdja, Y.Y.

Citation

Birdja, Y. Y. (2018, April 19). *Electrocatalytic CO₂ reduction toward liquid fuels : on heterogeneous electrocatalysts and heterogenized molecular catalysts*. Retrieved from <https://hdl.handle.net/1887/61513>

Version: Not Applicable (or Unknown)

License: [Licence agreement concerning inclusion of doctoral thesis in the Institutional Repository of the University of Leiden](#)

Downloaded from: <https://hdl.handle.net/1887/61513>

Note: To cite this publication please use the final published version (if applicable).

Cover Page



Universiteit Leiden



The handle <http://hdl.handle.net/1887/61513> holds various files of this Leiden University dissertation

Author: Birdja, Yuvraj Y.

Title: Electrocatalytic CO₂ reduction toward liquid fuels : on heterogeneous electrocatalysts and heterogenized molecular catalysts

Date: 2018-04-19

Advances and Challenges in the Electrocatalytic conversion of Carbon Dioxide to Fuels

This chapter is based on the article:

Yuvraj Y. Birdja, Elena Pérez-Gallent, Marta C. Figueiredo, Adrien J. Göttle, Federico Calle-Vallejo and Marc T. M. Koper, Nat. Energy, in preparation

Abstract

In this chapter, we critically review recent advances and relevant hurdles in the field of electrochemical CO₂ reduction. We start the discussion with the initial activation of CO₂ on the electrocatalyst, and its importance for the selectivity. Another mechanistic subject covered by this review, is the carbon-carbon bond formation from a mechanistic point of view. Additionally we discuss process- and reaction conditions, electrode mesoscale morphology, mass transport, and their influence on the electrocatalytic CO₂ reduction. Lastly, we discuss progress in two methodologies often used in CO₂ reduction research: in situ spectroscopic techniques and computational techniques.

2.1 Introduction

With the growing importance and falling prices of renewable electricity, the issue of electricity storage to deal with the intermittent nature of renewable energy sources is becoming urgent. The idea of storing renewable electricity into chemical bonds ("electrofuels") is particularly attractive, as it allows for high energy density and potentially high flexibility. While hydrogen is the most likely and realistic candidate for electricity storage in electrofuels, research into the electrochemical conversion of carbon dioxide and water into carbon-based fuels has intrigued electrochemists for many decades, and is currently undergoing a significant renaissance.^[1-4] In contrast to hydrogen production by water electrolysis, carbon dioxide electrolysis is still far from a mature technology. Significant hurdles regarding energy efficiency, reaction selectivity and overall conversion rate will need to be overcome if electrochemical carbon dioxide reduction is to become a viable option for storing (a part of) renewable electricity.

Several electrocatalysts have been reported for the production of different products from the electrocatalytic carbon dioxide reduction reaction (CO₂RR). Table 2.1 gives a selective overview of some of the most active and selective metal or metal-derived electrocatalysts towards specific products in aqueous media. The two-electron transfer products, CO and HCOOH, can be produced with low overpotential and high Faradaic efficiency (FE) on suitable electrocatalysts, but substantially higher overpotentials and lower selectivities are observed to multi-electron transfer products such as methane, ethylene and alcohols. For the ultimate goal of a high performance CO₂-electrolyzer in which CO₂ is being reduced to an electrofuel, only CO and HCOOH are currently potentially economically viable options to compete with the current (non-electrochemical) production processes.^[2]

There is no lack of reviews on the electrochemical reduction of CO₂; our own group has recently published an overview of the mechanistic aspects of CO₂RR electrocatalysts.^[5] The aim of this short review is not to be exhaustive, but rather to critically discuss some recent advances and pertinent challenges in this field, focusing on a few themes that have witnessed important progress in the recent literature.^[2,3,5,6] We have selected two mechanistic aspects to discuss. The initial activation of CO₂ on the electrocatalyst is key in determining the selectivity towards the first product, i.e. CO vs. HCOOH/HCOO⁻. Carbon-carbon bond formation is another mechanistic theme in CO₂RR which has received ample recent attention, especially on copper electrodes. It has also become increasingly clear from recent work that process and reaction conditions influence the CO₂RR significantly. While traditionally catalytic studies emphasize catalyst properties, CO₂RR activity and selectivity are very sensitive to electrolyte properties such as pH, cations, anions and solvent, as well as to mass transport conditions. Electrode morphology, especially on the mesoscale, is another topical theme in CO₂RR. Besides the themes mentioned, we will also discuss progress in two important methodologies, which are often used

Chapter 2. Advances and Challenges in the Electrocatalytic conversion of Carbon Dioxide to Fuels

to increase fundamental understanding of CO₂RR: in situ spectroscopic techniques and computational techniques.

Table 2.1 Some state-of-the-art electrocatalysts for specific CO₂RR products

CO ₂ RR product	Electrocatalyst	FE (%)	η (V)*	j_{total} (mA cm ⁻²)	Electrolyte (CO ₂ sat.)	Ref.
HCOOH	Pb	99.4	-1.19 V	5.0	0.1 M KHCO ₃ [∇]	[7]
	Sn	88.4	-1.04 V	5.0	0.1 M KHCO ₃ [∇]	[7]
	Pd _{nanopart.} \C	99	-0.15 V	2.4-7	2.8 M KHCO ₃ [⊥]	[8]
	Pd ₇₀ Pt _{30, nanopart.} \C	90	-0.36 V	4-7.5	0.2 M PO ₄ ³⁻ buffer [†]	[9]
CO	Au	87.1	-0.64 V	5.0	0.1 M KHCO ₃ [∇]	[7]
	Au _{nanopart.}	97	-0.58 V	3.49±0.61	0.1 M KHCO ₃ [∇]	[10]
	OD-Au _{nanopart.}	>96	-0.25 V	2-4	0.5 M NaHCO ₃ [◇]	[11]
	Ag	94	-0.99 V	≈5.0	0.1 M KHCO ₃ [∇]	[12]
CH ₄	Cu poly	40.4	-1.34 V	≈7	0.1 M KHCO ₃ [∇]	[13]
	Cu(210)	64	-1.29 V	5	0.1 M KHCO ₃ [∇]	[14]
C ₂ H ₄	Cu poly	26.0	-1.13 V	1-2	0.1 M KHCO ₃ [∇]	[13]
	Cu (<i>O₂ plasma tr.</i>)	60	-0.98 V	≈15	0.1 M KHCO ₃ [∇]	[15]
	Cu-halide	60.5-79.5	-2.11 V	46.1-39.2	3 M KBr [∠]	[16]
CH ₃ OH	Cu ₂ O	38	-0.34 V	1-2	0.5 M KHCO ₃ [‡]	[17]
	HCl-pretreated Mo	84	-0.33 V	0.12	0.2 M Na ₂ SO ₄ [⊤]	[18]
C ₂ H ₅ OH	Cu poly	9.8	-1.14 V	≈0.6	0.1 M KHCO ₃ [∇]	[13]
	Cu ₂ O	9-16	-1.08 V	30-35	0.1 M KHCO ₃ [∇]	[19]
	CuO _{nanopart.}	36.1	N/A ⁺	≈11.7	0.2 M KI	[20]
	Cu/CNS	63	-1.29 V	2	0.1 M KHCO ₃ [∇]	[21]

* E₀ vs. RHE from reference [5]; [∇] pH ≈ 6.8; [⊥] pH ≈ 8.2; [†] pH ≈ 6.7; [◇] pH ≈ 7.2; [∠] pH ≈ 3; [‡] pH ≈ 7.6; [⊤] pH ≈ 4.2; ⁺ at E = -1.7 V vs. SCE (pH not reported)

2.2 Initial activation of CO₂

The first step in any electrocatalytic reduction reaction of CO₂ is the initial activation of the CO₂ molecule. It is often claimed that activation and reduction of CO₂ is difficult, because the first electron transfer to form the CO₂^{•-} radical intermediate has a very negative redox potential (-1.9 V vs. NHE), or because CO₂ is a very stable molecule.^[4,22] Neither statement is accurate. The electrocatalyst stabilizes the CO₂^{•-} radical or reaction intermediate by the formation of a chemical bond, leading to a less negative redox potential. With the right electrocatalyst, it is possible to reduce CO₂ to CO or HCOOH at very low overpotential, which is related to the mechanism of a two-electron process, typically consisting of only one intermediate, which is relatively easily optimized.^[7,9] Enzymes such as formate dehydrogenase and carbon monoxide dehydrogenase are indeed effective reversible catalysts for the electrocatalytic conversion of CO₂ to formate and carbon monoxide (and vice versa), respectively, exhibiting negligible overpotentials.^[23]

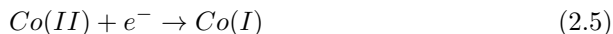
We consider four redox reactions related to the activation of CO₂ (eq. 2.1-2.4):



Eq. 2.1 and 2.2 are proton-coupled electron transfer (PCET) reactions and have been considered in a recent computational study by Studt et al. for deriving trends in selectivity among (post-)transition metal surfaces.^[24] They argued that *COOH is the more likely first intermediate for CO formation, and *OCHO the more likely intermediate for the formation of formic acid (an assertion that is generally agreed upon in the literature). Using calculated binding energies, they generally find good agreement between their predictions and experiment: post-transition metals such Pb and Sn prefer to bind via the oxygen and are selective towards formic acid, whereas transition metal electrodes prefer to bind via the carbon. Interestingly, in two instances their calculations deviate from the experimental observations in Table 2.1: silver is predicted to be an excellent catalyst for the formation of formic acid, whereas palladium is predicted to have the lowest onset potential for the formation of CO. They ascribe these differences to kinetic effects not included in their calculations. Interestingly, in the molecular electrocatalysis community the views on the initial activation of CO₂ appear to be subtly different. The initial binding of CO₂ to the catalyst does not involve a CPET step such as Eq. 2.1 and 2.2, both rather an electron-transfer mediated CO₂ binding step, as indicated by eq. 2.3. The CO₂⁻ anion adduct is generally bound to the metal center of the catalyst.

Chapter 2. Advances and Challenges in the Electrocatalytic conversion of Carbon Dioxide to Fuels

For instance, for a cobalt-(proto)porphyrin catalyst, CO₂ binding takes place if the cobalt center changes oxidation state from Co(II) to Co(I), with the electronic density flowing onto the *CO₂ ligand, formally written as in Eq. 2.5 and 2.6:



Subsequent protonation or CPET steps then generate the *COOH or *COOH⁻ intermediates. If this step is rate-determining, the pH dependence of CO₂ activation may differ from the pH dependence of the competing HER, which is confirmed by DFT calculations.^[25] Shen et al. used this different pH dependence of the CO₂RR and HER pathways to explain the strong pH dependence of the overall product selectivity on graphite-immobilized Co-protoporphyrin, with H₂ being the primary product at pH = 1 but CO being the primary product at pH = 3.^[26] Theoretical work showed that CO₂RR proceeds through different metal coordinated CO₂⁻ intermediates leading to either CO or HCOOH, similar to different binding modes of CO₂^{•-} on metal electrodes.^[27] A very similar mechanistic model was proposed by Wuttig et al. for the gold-catalyzed CO₂RR, suggesting that also on gold the *CO₂⁻ intermediate, and not *COOH, is the relevant activated form of CO₂.^[28] Recent computational work by Chen et al. has confirmed that on Ag(111), adsorbed CO₂ is highly sensitive to the presence of an electric field, as e.g. modeled by the presence of a cation.^[29] Although Chen et al. do not write the formation of *CO₂ as an electron-transfer step, the resulting *CO₂ is highly polarizable, and therefore sensitive to pH and cation effects (see section on Reaction- and Process Conditions).

A somewhat similar situation exists for the formation of formate/formic acid on molecular catalysts. Among the metal porphyrins, we recently showed that Rh, Sn and In protoporphyrins have a high selectivity towards formic acid in aqueous electrolyte.^[30] DFT calculations suggest that the key intermediate is an anionic hydride, formed through Eq. 2.4, as has been previously suggested in the molecular catalysis literature.^[31,32] The anionic hydride performs a nucleophilic attack of the carbon of the CO₂, yielding HCOO⁻. Again, the reaction is triggered by a potential-induced change in oxidation state of the catalyst, either of the metal center (in the case of Rh) or on the ligand (in the case of In and Sn). The stability of the resulting species is crucial to the subsequent elementary step and the formation of either CO or HCOOH/HCOO⁻. Interestingly, such a (lattice-)hydride mechanism was recently proposed for nanostructured copper-hydride catalysts with a much enhanced selectivity for formic acid ("normal" copper yields primarily CO as a two-electron product).^[33]

2.3 Carbon-carbon bond formation

One of the most interesting observations in the electrocatalytic reduction of CO_2 is the formation of species with one or more carbon-carbon bonds, which till date mostly has been reported for copper-based electrodes. Elucidation of the pathway(s) from CO_2 or CO to C_2 products has been the subject of several experimental^[14,34-38] and theoretical studies.^[39-43] Previous work from our group demonstrated the presence of two separate pathways for the formation of ethylene, each of which has a different intermediate: a surface insensitive pathway through a shared intermediate with the methane pathway, and a reaction path that takes place on $\text{Cu}(100)$ at low overpotential through an adsorbed CO dimer intermediate.^[36] This CO dimer intermediate has been proposed in several experimental^[34,37] and theoretical studies.^[39-41] DFT calculations have shown that the C-C coupling is only observed when a decoupled proton-electron transfer is assumed for the rate-determining steps,^[39] and not when CPET is assumed for every step in the mechanism.^[43,44] Moreover, the CO dimer configuration was found to be energetically feasible only when a charged water layer is taken into account,^[40] and the activation energy for its formation is more favorable on $\text{Cu}(100)$ compared to $\text{Cu}(111)$,^[40,42] in agreement with experimental observations. Although Wuttig et al.^[38] could not find spectroscopic signature of adsorbed OCCO and CHO species, they could not conclusively rule out the possibility of these or other surface species to be formed from COads, due to obscurity of OCCO by (bi)carbonate desorption and possible lower C-O oscillator strengths in case of CHO species. Recently, Pérez-Gallent et al.^[45] have provided evidence for a hydrogenated CO dimer intermediate (OCCOH) at low overpotentials in LiOH electrolyte during CO reduction using FTIR spectroscopy supported with density functional theory (DFT) calculations. The vibrational bands of 1191 and 1584 cm^{-1} observed during the reduction of CO , were assigned to the C-O-H and C=O stretching modes of this hydrogenated dimer intermediate, which was found to be structure sensitive, since its formation was only observed on $\text{Cu}(100)$ and not on $\text{Cu}(111)$, in agreement with previous studies.^[35,42]

Besides ethylene, other valuable C_2 products are acetaldehyde and ethanol. These three C_2 species are formed through common intermediates on $\text{Cu}(100)$ up to a selectivity-determining intermediate, the hydrogenation of which is inclined towards ethylene.^[39] However, ethanol formation is more favorable on undercoordinated copper sites,^[46] unlike ethylene formation, which prefers pristine (100) terraces.^[37,42]

Although the formation of higher order (C_{3+}) hydrocarbons is rarely observed, some studies have reported the formation of these products to occur via C-C coupling as well. C-C coupling between CO and C_2H_4 precursors has been reported to form n-propanol on agglomerates of oxide-derived copper nanocrystals.^[47] For this mechanism, the defect sites are proposed to be the catalytic active sites. Moreover, polymerization of adsorbed $-\text{CH}_2$ species has been proposed as mechanism for the formation of higher order hydrocarbons on bimetallic PdAu electrodes.^[48]

2.4 Reaction- and Process conditions

The influence of electrolyte composition, process- and reaction conditions has been acknowledged since the early experiments on CO₂RR.^[16,49–51] The nature of the electrolyte (aqueous or non-aqueous), pH, the identity of ionic species, or a combination of these factors, all influence the activity or selectivity of CO₂RR. However, the interpretation of these effects has remained poorly understood, and only recently systematic work has been performed to understand these effects.^[52–54] Moreover, other phenomena have been highlighted recently, such as the influence of local pH, buffering strength and mass transport^[55–58] as well as the existence and influence of homogeneously catalyzed chemical reactions during the CO₂RR.^[59,60]

Previously the influence of the electrolyte was investigated in terms of different (bulk) pH or ionic species.^[50,51] The interpretation of the effects of the aqueous electrolyte, ionic species and pH is complicated by a complex interplay of several of these factors, which makes it hard to ascribe a certain effect to a single parameter. Firstly, there has been controversy about the real active intermediate during CO₂ reduction. Most authors acknowledge that dissolved CO₂ is the active species, whereas some cases of bicarbonate as active species especially towards formate have been reported.^[61–63] The settlement of the H₂CO₃/HCO₃[–] equilibrium in water complicates conclusive statements about the role of bicarbonate on formate formation, which would ideally require in situ measurement of local concentrations of bicarbonate and formate during voltammetry. Secondly, the (bulk) pH, electrolyte composition and buffer capacity influence the concentrations of the carbonaceous species in solution^[64] and selectivity of CO₂RR.^[52,65] Recently, enhanced CO₂RR activity in bicarbonate electrolyte compared to other electrolytes under similar conditions, was proposed to be associated with the formation of a bicarbonate-CO₂ complex leading to an increase in effective CO₂ concentration in vicinity of the electrode.^[66] The authors claim that bicarbonate is the primary source of carbon in the formation of CO on gold, and generalize this role of bicarbonate to all CO-producing electrocatalysts. On the other hand, Wuttig et al. conclude that bicarbonate is not explicitly involved in the rate-limiting step of CO formation on gold.^[67] Instead, bicarbonate acts as a proton donor past the rate-limiting step, and as a sluggish buffer solution maintaining the bulk pH.

Additionally, the influence of the electrolyte can be associated with the presence of cationic or anionic species as was discovered by Hori and coworkers.^[49,50] Several research groups have reported cation effects on CO₂RR, where larger cations usually favor CO₂RR and the C₂/C₁ ratio. Till date there are in principle two explanations to rationalize this cation effect. On one hand, the degree of cation hydration is proposed to play a role.^[50,68,69] The cations differ in outer Helmholtz plane (OHP) potential, which leads to different local proton and CO₂ concentrations and subsequently different product selectivity for CO₂RR. On the other hand, the stabilization of the negatively charged intermediate by the cation has been proposed.^[29,70] The onset potential for ethylene depends on the cation nature,

while for methane no correlation has been found with cation size. This trend is in agreement with the observation of a hydrogenated dimer intermediate (OCCOH) only with smaller cations. This hydrogenated dimer is the key intermediate for the C-C coupling as discussed in the previous section.^[45]

The effect of anions on the CO₂RR has been investigated in the literature, although less extensively compared to cations, and the studies generally consist of halide effects on copper electrodes.^[16,51,53] These effects are generally explained in terms of halide adsorption on the catalyst surface, altering the electronic structure and subsequently the CO₂RR activity and selectivity, which are also dependent on the halide size and concentration.^[53] Moreover, specifically adsorbed halide anions can suppress proton adsorption, favoring CO₂RR with respect to HER.^[51]

Apart from bulk pH effects, the importance of the pH gradients and local pH has been the subject of several studies recently.^[55,56] It is generally known that during CO₂RR, an alkaline pH is manifested in the vicinity of the electrode, as result of proton consumption and hydroxide formation under cathodic conditions. This local pH change is proportional to the current density.^[71] The concentration of the electrolyte, in particular, the buffer capacity plays an important role on the local pH near the electrode. Moreover, the electrode morphology may also induce variations in the local pH, which can alter the product selectivity, as mentioned in a previous section. On Cu electrocatalysts, the selectivity toward ethylene can be favored by lowering the buffer capacity or by changing the electrode structure to obtain high current densities and thereby a high local pH.^[56] Additionally, the selectivity can be steered toward ethylene by increasing the CO₂ pressure, leading to enhanced local CO concentration and CO coverage. Although a different product spectrum was observed under similar conditions, Varela et al.^[55] reported similar conclusions regarding the effect of buffer capacity and local pH on the product selectivity of CO₂RR on Cu electrodes. The difference in product spectrum was presumed to be a result of different electrode morphology. In addition to properties indirectly affecting the mass transport of protons or CO₂ (electrode morphology, buffer capacity, etc.), forced or controlled mass transport also have been shown to influence the product selectivity of CO₂RR.^[57,58] Improved mass transport is generally associated with local pH approximating the bulk pH and enhanced local CO₂ concentration. However, improved mass transport does not necessarily lead to increased activity or selectivity of CO₂RR, since it may affect the competing HER as well. Rotating disc or cylinder experiments on Cu have shown that CO₂RR activity decreases with higher rotation rate, while HER activity increases together with a change in selectivity from CH₄ to CO.^[58] Recently, it was found that direct water reduction is the HER pathway in competition with CO₂RR instead of proton reduction, which is diffusion-limited at an acidic pH of 2.5.^[57] The suppression of water reduction is the result of adsorbed CO on the copper electrode and is more pronounced at low rotation rates (< 500 rpm). CO₂RR was found to be less sensitive to transport limitations compared to HER.^[72]

Another consequence of a local alkaline pH as result of the concomitant HER during CO₂RR, is the occurrence of chemical reactions, which may be homoge-

neously catalyzed.^[59,60] We recently found that Cannizzaro-type reactions can take place during CO₂RR, where aldehydes disproportionate into their corresponding carboxylic acid and primary alcohol.^[60] This phenomenon is catalyzed by the local alkaline pH near the electrode, and is therefore important in poorly buffered and unbuffered electrolytes. The obtained products (acids and alcohols) should be distinguished from direct CO₂ reduction products. This work will be discussed in chapter 3.

2.5 Electrode morphology and (sub)surface atoms

Besides the chemical nature of the electrocatalyst, the electrode morphology has been widely studied with the aim to understand and enhance CO₂RR activity and selectivity. Examples include different single crystals which have been the subject of previous research.^[14] More recently nano-^[73-77] and mesostructured^[72,78-81] catalysts and oxide-derived electrodes^[82-87] have shown interesting properties influencing the CO₂RR activity and selectivity such as coordination number of active sites, particle size, readsorption of intermediates, interparticle distance and transport phenomena.

Rough or high surface-area surfaces such as copper nanoparticles have been shown to exhibit improved hydrocarbon selectivity compared with smooth surfaces, due to increased population of undercoordinated sites.^[73] Cubic shaped copper nanocrystals are able to steer the selectivity towards ethylene with respect to methane.^[74] The surface structure consists mainly of (100) facets, which is presumed to be key for the high C₂/C₁ ratio. Similar results were obtained by Loiudice et al.,^[75] who reported an optimal cube size due to a balance between edge- and plane sites. Another type of roughened electrodes, copper nanofoams, turned out to increase faradaic efficiency towards formic acid at the expense of CH₄ and C₂H₄, and to form propylene.^[76]

In addition to specific sites of nanoparticles, a particle size effect of Cu nanoparticles has been reported,^[77] in which the authors showed that the activity for H₂ and CO is increased with decreasing particle size (< 5 nm), while the selectivity towards hydrocarbons is decreased. This observation was attributed to higher amount of undercoordinated sites (CN < 8), which promote HER and CO formation due to stronger chemisorption of the CO intermediate. Since different synthesis methods of Cu nanoparticles and experimental conditions for CO₂ reduction were used, it is hard to generalize the results of these studies in terms of morphology effects of Cu nanoparticles.

Apart from the nanostructure, more recently the mesostructure of copper electrodes also has been shown to play an important role in the product selectivity of C₁ vs. C₂ products. The local pH and retention time of key intermediates inside the pores of mesoporous Cu electrodes can be altered, steering the selectivity towards ethane and ethylene.^[78] Chen et al.^[79] reported robust Cu mesocrystals, prepared by in situ reduction of CuCl thin films during CO₂RR, which exhibit high activity and stability toward ethylene (C₂H₄/CH₄ ≈ 18) at -0.99 V vs. RHE. These mesocrystals

2.5. Electrode morphology and (sub)surface atoms

exhibit Cu(100) facets and steps, contrary to regular Cu nanoparticles or Cu foils, and CO adsorption is preferred on these sites, leading to high faradaic efficiency towards C_2H_4 on the Cu mesocrystals. Investigation of mesoscale phenomena have demonstrated the effects of particle size and distance on the product selectivity for well-defined Cu catalysts.^[80] Readsorption of the CO intermediates, followed by their further reduction is found to be associated with small interparticle distance and larger nanoparticle sizes, whereas small nanoparticles suffer from poisoning of active sites by CO. Control of these mesoscale parameters could be used to tune the selectivity of CO_2RR . The role of the mesostructure on the selectivity has also been shown on gold electrodes.^[72] Hydrogen evolution was shown to be suppressed by increasing the porosity of the electrode, while CO_2RR is more resistant to transport limitations caused by porous electrodes. On a similar note, it was found that efficient CO_2 transport on porous Cu hollow fibre electrodes, which exhibit many defect sites, increases CO selectivity.^[81]

In 2012, research conducted by Kanan and coworkers revealed the increased energetic efficiency and stability of CO_2RR on oxide-derived (OD) electrocatalysts, which were obtained by reducing metal-oxide films. Improved CO_2RR activity has been reported for e.g. OD gold, OD copper and OD lead.^[11,82,83] To date there are various other papers published regarding CO_2/CO reduction on OD copper electrodes,^[84–87] but the key factor responsible for the improved selectivity and activity of oxide-derived electrocatalysts is still unclear. In this respect, increased stabilization of the CO_2 anion radical ($CO_2^{\bullet-}$) by grain boundaries and (sub)surface oxygen or oxidized species have been reported to play a role, although no consensus has been reached to date.^[88–90]

On OD Au, high selectivity to CO at low overpotential was found, which was ascribed to improved stabilization of $CO_2^{\bullet-}$ on the OD Au compared to polycrystalline Au.^[11] Similar conclusion has been drawn for OD Cu for the formation of CO.^[85] Additionally, on copper the enhanced activity and stability compared to polycrystalline Cu depend on the initial thickness of the Cu_2O layers and is not significant for thin films ($< 3 \mu m$).^[82,86] Later, remarkable improvement of the selectivity toward ethanol, acetate and n-propanol for CO reduction on similar electrodes, was reported.^[87] The authors exclude the influence of nanocrystallite size or morphology on the enhanced CO activity, and associate the improved selectivity with grain boundaries instead, facilitating strong CO binding sites.^[88,89]

Eilert et al.^[90] demonstrated the role of subsurface oxygen in the oxide-derived copper electrocatalysts by in situ ambient pressure XPS and quasi in situ EELS in a transmission electron microscope. They proposed that subsurface oxygen modifies the electrocatalyst's electronic structure by reducing σ -repulsion, leading to increased CO binding energies, and consequently higher CO coverage, which promotes C_2 selectivity. The authors assumed that influence of grain boundaries in the oxide-derived Cu, as discussed before, originated from residual oxygen present in the subsurface. Key in this mechanism was the presence of near-surface sites, which inhibited diffusion of subsurface oxygen to the surface and thereby protonation to form water. DFT calculations have shown that interstitial oxygen species are stable

at Cu(111) subsurface, contrary to Cu(211), and are capable of improving CO₂ binding to the surface.^[91]

When Cu_xO is used directly for CO₂RR, methanol,^[17,92] ethanol,^[19,20] and ethylene^[19] were observed as major products. It is often assumed that during CO₂RR, the Cu_xO electrocatalyst should be completely converted to metallic Cu. However, Lee and coworkers^[93] showed that a residual oxide layer remains present on the surface during CO₂RR and they proposed the surface oxide and OD-metallic layer as key reaction sites for catalysis. They also reported the formation of C₃-C₄ products due to a synergistic effect between Cu₂O and Cl adsorption, which resulted in a higher population of Cu⁺ species.^[94] Similar results were obtained by Mistry et al.,^[15] who showed that Cu⁺ species are resistant to reduction and considered the active species for improved selectivity toward ethylene. The role of Cu⁺ was contradicted by Xiao et al.,^[95] who demonstrate a synergistic effect of surface Cu⁺ and Cu⁰, which improves the CO₂ activation and CO dimerization. Individual Cu⁺ species affect the CO₂RR efficiency and selectivity negatively. The presence of both, surface Cu⁺ and Cu⁰, can be caused by subsurface oxygen,^[96] which is in agreement with the importance of subsurface oxygen discussed in the previous paragraph.

2.6 In situ spectroscopic investigation of CO₂ reduction

In situ spectroscopy techniques can provide very useful information about electrocatalytic reactions such as reaction intermediates adsorbed on the electrode surface, and dissolved species involved in the reaction. The technique most often used is FTIR spectroscopy. A general review on in situ FTIR spectroelectrochemistry was given by Ye et al.^[97] Major bottlenecks related to external reflection FTIR are the high ohmic resistance in the thin layer solution, hindered mass transport conditions, and interference due to infrared absorption from bulk water. Another often used spectroelectrochemical technique is Surface enhanced Raman spectroscopy (SERS), which provides very sensitive characterization of adsorbed species at the electrode surface. A drawback of SERS is the local enhancement of spectroscopic signals which leads to a relatively biased representation of the electrode surface as you only see the "hotspots". Osawa et al.^[98] showed that surface enhanced absorption spectroscopy (SEIRAS) in an attenuated total reflection (ATR) configuration may solve the aforementioned limitations of FTIR and SERS. More recently, some studies have utilized in situ x-ray absorption spectroscopy (XAS) to characterize the surface during CO₂RR aimed at pinpointing the active catalytic species. Here we briefly discuss recent in situ spectroscopic studies that have revealed novel insight on the electrochemical CO₂ reduction.

During CO₂RR, gaseous products such as CO, and H₂ from the concomitant hydrogen evolution in aqueous media negatively affect the spectroscopic measurement due to bubble formation. For this reason, most of the early studies concerning

2.6. In situ spectroscopic investigation of CO₂ reduction

FTIR of CO₂ electrochemical reduction were performed in non-aqueous solutions, avoiding hydrogen evolution. Recently, Figueiredo et al.^[99] showed the high sensitivity of CO₂ reduction to the presence of residual water in acetonitrile using in situ FTIR and SERS. They showed that in non-dry conditions adsorbed CO is the major product at low overpotentials, and that (bi)carbonates are formed at Cu, Pt, Au, Pd and Ag electrodes from the chemical conversion of CO₂ by a significantly high concentration of OH⁻ species formed from water reduction. As a consequence, (bi)carbonate formation was found to be proportional to the water content. The formation of oxalate was only observed for Pb electrodes at extremely high overpotentials.

The formation of the higher order hydrocarbons on Cu electrodes proceeds via an adsorbed CO species, although the rate-limiting step is not agreed upon by experimental^[4,5,13,34,37] and theoretical^[39-41,43,100] studies. Wuttig and coworkers^[38] utilized SEIRAS to reveal that adsorbed CO species are bound to the electrode surface at potentials < -0.60 V vs. RHE, independent of pH, but weakly dependent on the potential. Spectroscopic studies shed light on the concerted or sequential nature of proton- and electron transfer pathways related to CO₂RR on various electrodes.^[28,101] In situ ATR-SEIRAS revealed the fundamentally different proton coupling behavior between CO₂ reduction and hydrogen evolution reaction (HER), which plays an important role in the selectivity toward CO vs. H₂ on gold.^[28] The authors in this work reported a rate-limiting single electron transfer (ET) to CO₂, which was decoupled from proton transfer (PT) from hydronium, bicarbonate or carbonic acid. In contrast, PT from these species was rate limiting for the HER, leading to H_{ads}. The vibrational band between $\approx 1900 - 2050 \text{ cm}^{-1}$, ascribed to CO adsorbed on Au bridge sites, was argued by Dunwell et al.^[66] to be the result of Pt deposition of the counter electrode on the Au working electrode.

Another aspect often studied with in situ spectroscopy is the (change in) surface structure during CO₂RR. Pander et al.^[102] investigated the role of metastable surface oxides for CO₂ reduction on tin, indium, lead and bismuth electrodes, by means of ATR-IR. The results indicate the competition between CO₂ and H⁺ for reaction sites (oxidized or metallic sites), depending on the nature of the electrode. Very recently, ATR-IR and SERS have also been utilized to indirectly monitor (reconstruction of) the surface during CO₂RR.^[103] Moreover, the oxide derived catalysts (as discussed in the previous section) have been probed by XAS^[15,93,104] and ambient pressure XPS^[90] in order to gain insight in the chemical state of the active (Cu) species.

As discussed, spectroscopic studies of electrochemical CO₂ reduction provide information of high importance for the better understanding of the reaction intermediates and products. Yet, the number of studies, especially concerning in situ XAS and XPS, is still limited, and the opportunities for following studies and technical development is very wide.

2.7 Computational approaches for CO₂ reduction

Over the last decades, computational electrochemistry has increased in importance to predict, explain or support the outcome of experiments. Density Functional Theory (DFT) calculations applied to the electrode/electrolyte interface is a far from simple endeavor, but much progress has been made in improving models. A review of the achievements and challenges within first-principles computational electrochemistry is given by Calle-Vallejo et al.,^[105] and a more comprehensive review on multiscale simulations from the atomic to the system scale can be found elsewhere.^[106] In this section, we will limit ourselves to recent advances and key scientific challenges of computational approaches with respect to the electrocatalytic reduction of CO₂ and CO.

Since its introduction by Nørskov et al.,^[107] the computational hydrogen electrode (CHE) has been widely employed for computations in electrocatalysis, in particular for CO₂ and CO electroreduction. Using this model together with DFT to calculate the adsorption energies of the intermediates, one can gain mechanistic insight in the possible reaction pathways, and can estimate the potentials at which the redox reactions take place.^[39,100,108] However, models based on the CHE typically assume concerted proton-coupled electron transfer steps (CPET), and are therefore not fully applicable for reaction pathways where decoupled proton- and electron transfer steps are involved. Sequential proton-electron transfer (SPET) steps have been observed on molecular and oxide electrocatalysts, as well as on metallic electrocatalysts, making them pH sensitive.^[5,109,110] Recently, a simple methodology was introduced that allows to predict the transition between coupled and decoupled proton-electron transfer pathways^[25] based on the accurate calculation of acid-base equilibrium constants.^[111] Using this methodology, the experimental pH dependence of CO₂ reduction on immobilized cobalt protoporphyrin IX has been rationalized.^[26]

The presence of linear correlations between adsorption energies of similar adsorbates, known as scaling relations,^[112] is advantageous for reducing the complexity of DFT-based catalytic models and facilitate the simultaneous analysis of numerous materials. However, these scaling relations pose extra constraints for finding optimal electrocatalysts with low overpotentials, and are therefore extensively studied.^[113–115] There have been various recent efforts undertaken to break or circumvent scaling relations, especially between the intermediates of the electrocatalytic OER, ORR and CO₂RR.^[42,116,117] The strategy is clear, although in practice difficult to implement experimentally: one of the intermediates needs to be significantly stabilized with respect to the other. For instance, the preference of Cu(100) for the production of ethylene and ethanol over methane has been explained on the basis of the breaking of scaling relations between adsorbed CO and CO dimers on that facet due to strong ensemble effects upon CO dimerization.^[42] Another example is the nearly reversible reduction of CO₂ to CO on CODH enzymes, the active site of which does not obey the scaling relationship between adsorbed CO and COOH.^[118] Furthermore, Li and Sun^[119] and Peterson and Nørskov^[108] discussed

several strategies in this respect for CO₂RR: tuning of metal surfaces such as to obtain low-coordination sites and introduction of p-block dopants or oxophilic sites. Other ways to depart from scaling relations are the modification of the electrolyte composition,^[116] anchoring active ligands on the surface or at the active sites,^[120] the search for transition-metal-free electrocatalysts and the decoupling of PT and ET transfers.

As mentioned before, much work has been devoted to copper electrodes, because of their ability to produce hydrocarbons and alcohols in significant quantities. DFT studies have been mainly carried out to propose reaction pathways and to explain the selectivity on different electrocatalysts or surface sites. Durand et al.^[121] showed that the stability of the key intermediates increases in the order Cu(111) < Cu(100) < Cu(211), which implies that the preferred sites for hydrocarbon formation on copper are low-coordination sites such as steps and kinks.^[121,122] Note that CHE-based models do not generally incorporate reaction barriers, which is another important topic under study in CO₂ and CO electroreduction.^[123,124] Nie et al.^[43] showed the importance of elementary step kinetics on the mechanism of CO₂ reduction to C₁ products. Formation of either a CHO or COH adsorbed intermediate from CO hydrogenation determines the selectivity on Cu(111). CH_x species are formed via the more kinetically favorable COH intermediate, which eventually leads to methane and ethylene. However, when only reaction free energies are taken into account, the lowest-energy pathway to methane/methanol would be through a CHO intermediate, as reported by Peterson et al.^[100]

Recently, Xiao et al.^[125] argued that adsorbate solvation is not (sufficiently) taken into account in the previous studies by Nie et al.^[43] and Montoya et al.,^[40] and proposed a mechanism on Cu(111) where surface water is claimed to influence the selectivity towards hydrocarbons compared to alcohol products. The modeling of solvation is crucial when attempts are made to break scaling relations and is often overlooked or taken into account as a constant correction to the adsorption energies calculated in vacuum.^[39,100,107,108] However, it was recently found that solvation restores the scalability broken under vacuum.^[116]

In summary, significant progress has been made in the past few years towards a comprehensive understanding of CO₂/CO electroreduction. Numerous challenges still lie ahead, which currently prevent the development of accurate materials screening routines for the design of new CO₂/CO reduction materials.^[126] To date, there are no reports of *in silico* designed catalysts for CO₂/CO reduction that have been successfully implemented experimentally. We hope that future advances in pH- and potential-dependent reaction barriers, solvation and scaling relations will enable such developments.

2.8 Future directions and perspectives

Electrocatalytic CO₂ reduction is considered a potential means to alleviate CO₂ accumulation in the atmosphere, and store intermittent renewable energy in elec-

trofuels. In order to verily contribute to a sustainable carbon cycle, large-scale implementation of this process is eventually needed. In the last few decades significant progress has been made mainly regarding the design of highly active or selective electrocatalysts, and their mechanism for CO₂RR. However, it is of crucial importance to realize the importance of other related aspects discussed in this review, electrode morphology, (sub)surface structure, reaction- and process conditions, not only from a mechanistic point of view, but from an engineering perspective as well. Particularly, not only the electrode/electrolyte interface should be studied, but transport phenomena, catalyst stability and electrolyte/solvent effects should be optimized as well. In this endeavor it is desired and even necessary to combine computational and in situ spectroelectrochemical techniques. Ideally one would like to combine all the different parameters in a (computational) model instead of a theoretical model that provides only (mechanistic) information for a specific case limited by various boundary conditions. We believe that future CO₂RR research should deviate from solely finding or improving highly active/selective electrocatalysts, and rather should focus on the joint action of all relevant aspects in order to become a viable option for the production of electrofuels.

2.9 References

- [1] D. T. Whipple, P. J. A. Kenis, *J. Phys. Chem. Lett.* **2010**, *1*, 3451–3458.
- [2] J. Durst, A. Rudnev, A. Dutta, Y. Fu, J. Herranz, V. Kaliginedi, A. Kuzume, A. A. Permyakova, Y. Paratcha, P. Broekmann, T. J. Schmidt, *Chimia* **2015**, *69*, 769–776.
- [3] J.-P. Jones, G. K. S. Prakash, G. A. Olah, *Isr. J. Chem.* **2014**, *54*, 1451–1466.
- [4] Y. Hori, *In Modern Aspects of Electrochemistry Vol. 42*, Springer, New York, **2008**.
- [5] R. Kortlever, J. Shen, K. J. P. Schouten, F. Calle-Vallejo, M. T. M. Koper, *J. Phys. Chem. Lett.* **2015**, *6*, 4073–4082.
- [6] Z. W. Seh, J. Kibsgaard, C. F. Dickens, I. Chorkendorff, J. K. Nørskov, T. F. Jaramillo, *Science* **2017**, *355*, eaad4998.
- [7] Y. Hori, H. Wakebe, T. Tsukamoto, O. Koga, *Electrochim. Acta* **1994**, *39*, 1833–1839.
- [8] X. Min, M. W. Kanan, *J. Am. Chem. Soc.* **2015**, *137*, 4701–4708.
- [9] R. Kortlever, I. Peters, S. Koper, M. T. M. Koper, *ACS Catal.* **2015**, *5*, 3916–3923.
- [10] E. R. Cave, J. H. Montoya, K. P. Kuhl, D. N. Abram, T. Hatsukade, C. Shi, C. Hahn, J. K. Nørskov, T. F. Jaramillo, *Phys. Chem. Chem. Phys.* **2017**, *19*, 15856–15863.

- [11] Y. Chen, C. W. Li, M. W. Kanan, *J. Am. Chem. Soc.* **2012**, *134*, 19969–19972.
- [12] T. Hatsukade, K. P. Kuhl, E. R. Cave, D. N. Abram, T. F. Jaramillo, *Phys. Chem. Chem. Phys.* **2014**, *16*, 13814–13819.
- [13] K. P. Kuhl, E. R. Cave, D. N. Abram, T. F. Jaramillo, *Energy Environ. Sci.* **2012**, *5*, 7050–7059.
- [14] Y. Hori, I. Takahashi, O. Koga, N. Hoshi, *J. Mol. Catal. A: Chem.* **2003**, *199*, 39–47.
- [15] H. Mistry, A. S. Varela, C. S. Bonifacio, I. Zegkinoglou, I. Sinev, Y.-W. Choi, K. Kisslinger, E. A. Stach, J. C. Yang, P. Strasser, B. R. Cuenya, *Nat. Commun.* **2016**, *7*, 12123.
- [16] H. Yano, T. Tanaka, M. Nakayama, K. Ogura, *J. Electroanal. Chem.* **2004**, *565*, 287–293.
- [17] M. Le, M. Ren, Z. Zhang, P. T. Sprunger, R. L. Kurtz, J. C. Flake, *J. Electrochem. Soc.* **2011**, *158*, E45–E49.
- [18] K. W. Frese Jr., S. C. Leach, D. P. Summers, *US4609441A* **1986**.
- [19] D. Ren, Y. Deng, A. D. Handoko, C. S. Chen, S. Malkhandi, B. S. Yeo, *ACS Catal.* **2015**, *5*, 2814–2821.
- [20] D. Chi, H. Yang, Y. Du, T. Lv, G. Sui, H. Wang, J. Lu, *RCS Adv.* **2014**, *4*, 37329–37332.
- [21] Y. Song, R. Peng, D. K. Hensley, P. V. Bonnesen, L. Liang, Z. Wu, H. M. M. III, M. Chi, C. Ma, B. G. Sumpter, A. J. Rondinone, *ChemistrySelect* **2016**, *1*, 6055–6061.
- [22] E. E. Benson, C. P. Kubiak, A. J. Sathrum, J. M. Smieja, *Chem. Soc. Rev.* **2009**, *38*, 89–99.
- [23] F. A. Armstrong, J. Hirst, *Proc. Natl. Acad. Sci.* **2011**, *108*, 14049–14054.
- [24] J. S. Yoo, R. Christensen, T. Vegge, J. K. Nørskov, F. Studt, *ChemSusChem* **2016**, *9*, 358–363.
- [25] A. J. Göttle, M. T. M. Koper, *Chem. Sci.* **2017**, *8*, 458–465.
- [26] J. Shen, R. Kortlever, R. Kas, Y. Y. Birdja, O. Diaz-Morales, Y. Kwon, I. Ledezma-Yanez, K. J. P. Schouten, G. Mul, M. T. M. Koper, *Nat. Commun.* **2015**, *6*, 8177.
- [27] J. Shen, M. J. Kolb, A. J. Göttle, M. T. M. Koper, *J. Phys. Chem. C* **2016**, *120*, 15714–15721.
- [28] A. Wuttig, M. Yaguchi, K. Motobayashi, M. Osawa, Y. Surendranath, *Proc. Natl. Acad. Sci.* **2016**, *113*, E4585–E4593.
- [29] L. D. Chen, M. Urushihara, K. Chan, J. K. Nørskov, *ACS Catal.* **2016**, *6*, 7133–7139.

Chapter 2. Advances and Challenges in the Electrocatalytic conversion of Carbon Dioxide to Fuels

- [30] Y. Y. Birdja, J. Shen, M. T. M. Koper, *Catal. Today* **2017**, *288*, 37–47.
- [31] B. H. Solis, A. G. Maher, D. K. Dogutan, D. G. Nocera, S. Hammes-Schiffer, *Proc. Natl. Acad. Sci.* **2016**, *113*, 485–492.
- [32] A. J. Göttle, M. T. M. Koper, *J. Am. Chem. Soc.* **under revision**.
- [33] Q. Tang, Y. Lee, D.-Y. Li, W. Choi, C. W. Liu, D. Lee, D. en Jiang, *J. Am. Chem. Soc.* **2017**, *139*, 9728–9736.
- [34] K. J. P. Schouten, Y. Kwon, C. J. M. van der Ham, Z. Qin, M. T. M. Koper, *Chem. Sci.* **2011**, *2*, 1902–1909.
- [35] K. J. P. Schouten, E. P. Gallent, M. T. M. Koper, *ACS Catal.* **2013**, *3*, 1292–1295.
- [36] K. J. P. Schouten, Z. Qin, E. P. Gallent, M. T. M. Koper, *J. Am. Chem. Soc.* **2012**, *134*, 9864–9867.
- [37] M. Gattrell, N. Gupta, A. Co, *J. Electroanal. Chem.* **2006**, *594*, 1–19.
- [38] A. Wuttig, C. Liu, Q. Peng, M. Yaguchi, C. H. Hendon, K. Motobayashi, S. Ye, M. Osawa, Y. Surendranath, *ACS Cent. Sci.* **2016**, *2*, 522–528.
- [39] F. Calle-Vallejo, M. T. M. Koper, *Angew. Chem. Int. Ed.* **2013**, *52*, 7282–7285.
- [40] J. H. Montoya, C. Shi, K. Chan, J. K. Nørskov, *J. Phys. Chem. Lett.* **2015**, *6*, 2032–2037.
- [41] J. D. Goodpaster, A. T. Bell, M. Head-Gordon, *J. Phys. Chem. Lett.* **2016**, *7*, 1471–1477.
- [42] H. Li, Y. Li, M. T. M. Koper, F. Calle-Vallejo, *J. Am. Chem. Soc.* **2014**, *136*, 15694–15701.
- [43] X. Nie, M. R. Esopi, M. J. Janik, A. Asthagiri, *Angew. Chem. Int. Ed.* **2013**, *52*, 2459–2462.
- [44] J. H. Montoya, A. A. Peterson, J. K. Nørskov, *ChemCatChem* **2013**, *5*, 737–742.
- [45] E. Pérez-Gallent, M. C. Figueiredo, F. Calle-Vallejo, M. T. M. Koper, *Angew. Chem. Int. Ed.* **2017**, *56*, 3621–3624.
- [46] I. Ledezma-Yanez, E. P. Gallent, M. T. M. Koper, F. Calle-Vallejo, *Catal. Today* **2016**, *262*, 90–94.
- [47] D. Ren, N. T. Wong, A. D. Handoko, Y. Huang, B. S. Yeo, *J. Phys. Chem. Lett.* **2016**, *7*, 20–24.
- [48] R. Kortlever, I. Peters, C. Balemans, R. Kas, Y. Kwon, G. Mul, M. T. M. Koper, *Chem. Commun.* **2016**, *52*, 10229–10232.
- [49] Y. Hori, A. Murata, R. Takahashi, S. Suzuki, *J. Chem. Soc. Chem. Commun.* **1988**, *0*, 17–19.

- [50] A. Murata, Y. Hori, *Bull. Chem. Soc. Jpn.* **1991**, *64*, 123–127.
- [51] K. Ogura, J. R. Ferrell III, A. V. Cugini, E. S. Smotkin, M. D. Salazar-Villalpando, *Electrochim. Acta* **2010**, *56*, 381–386.
- [52] M. R. Singh, E. L. Clark, A. T. Bell, *Phys. Chem. Chem. Phys.* **2015**, *17*, 18924–18936.
- [53] A. S. Varela, W. Ju, T. Reier, P. Strasser, *ACS Catal.* **2016**, *6*, 2136–2144.
- [54] A. Schizodimou, G. Kyriacou, *Electrochim. Acta* **2012**, *78*, 171–176.
- [55] A. S. Varela, M. Kroschel, T. Reier, P. Strasser, *Catal. Today* **2016**, *260*, 8–13.
- [56] R. Kas, R. Kortlever, H. Yilmaz, M. T. M. Koper, G. Mul, *ChemElectroChem* **2015**, *2*, 354–358.
- [57] H. Ooka, M. C. Figueiredo, M. T. M. Koper, *Langmuir* **2017**, *33*, 9307–9313.
- [58] C. F. C. Lim, D. A. Harrington, A. T. Marshall, *Electrochim. Acta* **2017**, *238*, 56–63.
- [59] O. R. Luca, A. Q. Fenwick, *J. Photochem. Photobiol. B* **2015**, *152*, 26–42.
- [60] Y. Y. Birdja, M. T. M. Koper, *J. Am. Chem. Soc.* **2017**, *139*, 2030–2034.
- [61] Y. Hori, S. Suzuki, *J. Electrochem. Soc.* **1983**, *130*, 2387–2390.
- [62] B. Innocent, D. Pasquier, F. Ropital, F. Hahn, J.-M. Leger, K. Kokoh, *Appl. Catal. B: Environ.* **2010**, *94*, 219–224.
- [63] R. Kortlever, K. H. Tan, Y. Kwon, M. T. M. Koper, *J. Solid State Electrochem.* **2013**, *17*, 1843–1849.
- [64] H. Zhong, K. Fujii, Y. Nakano, F. Jin, *J. Phys. Chem. C* **2015**, *119*, 55–61.
- [65] N. Yoshihara, M. Arita, M. Noda, *Chem. Lett.* **2017**, *46*, 125–127.
- [66] M. Dunwell, Q. Lu, J. M. Heyes, J. Rosen, J. G. Chen, Y. Yan, F. Jiao, B. Xu, *J. Am. Chem. Soc.* **2017**, *139*, 3774–3783.
- [67] A. Wuttig, Y. Yoon, J. Ryu, Y. Surendranath, *J. Am. Chem. Soc.* **2017**, *139*, 17109–17113.
- [68] M. R. Singh, Y. Kwon, Y. Lum, I. Joel W. Ager, A. T. Bell, *J. Am. Chem. Soc.* **2016**, *138*, 13006–13012.
- [69] M. R. Thorson, K. I. Siil, P. J. A. Kenis, *J. Electrochem. Soc.* **2013**, *160*, F69–F74.
- [70] E. Pérez-Gallent, G. Marcandalli, M. C. Figueiredo, F. Calle-Vallejo, M. T. M. Koper, *J. Am. Chem. Soc.* **2017**, *139*, 16412–16419.
- [71] N. Gupta, M. Gattrell, B. Macdougall, *J. Appl. Electrochem.* **2006**, *36*, 161–172.
- [72] A. S. Hall, Y. Yoon, A. Wuttig, Y. Surendranath, *J. Am. Chem. Soc.* **2015**, *137*, 14834–14837.

- [73] W. Tang, A. A. Peterson, A. S. Varela, Z. P. Jovanov, L. Bech, W. J. Durand, S. Dahl, J. K. Nørskov, I. Chorkendorff, *Phys. Chem. Chem. Phys.* **2012**, *14*, 76–81.
- [74] F. S. Roberts, K. P. Kuhl, A. Nilsson, *Angew. Chem. Int. Ed.* **2015**, *54*, 5179–5182.
- [75] A. Loiudice, P. Lobaccaro, E. A. Kamali, T. Thao, B. H. Huang, J. W. Ager, R. Buonsanti, *Angew. Chem. Int. Ed.* **2016**, *55*, 5789–5792.
- [76] S. Sen, D. Liu, G. T. R. Palmore, *ACS Catal.* **2014**, *4*, 3091–3095.
- [77] R. Reske, H. Mistry, F. Behafarid, B. R. Cuenya, P. Strasser, *J. Am. Chem. Soc.* **2014**, *136*, 6978–6986.
- [78] K. D. Yang, W. R. Ko, J. H. Lee, S. J. Kim, H. Lee, M. H. Lee, K. T. Nam, *Angew. Chem. Int. Ed.* **2017**, *56*, 796–800.
- [79] C. S. Chen, A. D. Handoko, J. H. Wan, L. Ma, D. Ren, B. S. Yeo, *Catal. Sci. Technol.* **2015**, *5*, 161–168.
- [80] H. Mistry, F. Behafarid, R. Reske, A. S. Varela, P. Strasser, B. R. Cuenya, *ACS Catal.* **2016**, *6*, 1075–1080.
- [81] R. Kas, K. K. Hummadi, R. Kortlever, P. de Wit, A. Milbrat, M. W. Luiten-Olieman, N. E. Benes, M. T. Koper, G. Mul, *Nat. Commun.* **2016**, *7*, 10748.
- [82] C. W. Li, M. W. Kanan, *J. Am. Chem. Soc.* **2012**, *134*, 7231–7234.
- [83] C. H. Lee, M. W. Kanan, *ACS Catal.* **2015**, *5*, 465–469.
- [84] A. Dutta, M. Rahaman, N. C. Luedi, M. Mohos, P. Broekmann, *ACS Catal.* **2016**, *6*, 3804–3814.
- [85] M. Ma, K. Djanashvili, W. A. Smith, *Phys. Chem. Chem. Phys.* **2015**, *17*, 20861–20867.
- [86] R. Kas, R. Kortlever, A. Milbrat, M. T. M. Koper, G. Mul, J. Baltrusaitis, *Phys. Chem. Chem. Phys.* **2014**, *16*, 12194–12201.
- [87] C. W. Li, J. Ciston, M. W. Kanan, *Nature* **2014**, *508*, 504–507.
- [88] X. Feng, K. Jiang, S. Fan, M. W. Kanan, *ACS Cent. Sci.* **2016**, *2*, 169–174.
- [89] A. Verdaguier-Casadevall, C. W. Li, T. P. Johansson, S. B. Scott, J. T. McKeown, M. Kumar, I. E. L. Stephens, M. W. Kanan, I. Chorkendorff, *J. Am. Chem. Soc.* **2015**, *137*, 9808–9811.
- [90] A. Eilert, F. Cavalca, F. S. Roberts, J. Osterwalder, C. Liu, M. Favaro, E. J. Crumlin, H. Ogasawara, D. Friebe, L. G. M. Pettersson, A. Nilsson, *J. Phys. Chem. Lett.* **2017**, *8*, 285–290.
- [91] J. Xiao, A. Kuc, T. Frauenheim, T. Heine, *J. Mater. Chem. A* **2014**, *2*, 4885–4889.
- [92] K. W. Frese, Jr., *J. Electrochem. Soc.* **1991**, *138*, 3338–3344.

- [93] D. Kim, S. Lee, J. D. Ocon, B. Jeong, J. K. Lee, J. Lee, *Phys. Chem. Chem. Phys.* **2015**, *17*, 824–830.
- [94] S. Lee, D. Kim, J. Lee, *Angew. Chem. Int. Ed.* **2015**, *54*, 14701–14705.
- [95] H. Xiao, W. A. Goddard III, T. Cheng, Y. Liu, *Proc. Natl. Acad. Sci.* **2017**, *114*, 6685–6688.
- [96] M. Favaro, H. Xiao, T. Cheng, W. A. Goddard, J. Yano, E. J. Crumlin, *Proc. Natl. Acad. Sci.* **2017**, *114*, 6706–6711.
- [97] J.-Y. Ye, Y.-X. Jiang, T. Sheng, S.-G. Sun, *Nano Energy* **2016**, *29*, 414–427.
- [98] M. Osawa in *Diffraction and Spectroscopic Methods in Electrochemistry (Advances in Electrochemical Science and Engineering)*, Vol. 9, (Eds.: R. C. Alkire, D. M. Kolb, J. Lipkowski, P. N. Ross), Wiley-VCH, New York, NY, USA, **2006**, pp. 269–314.
- [99] M. C. Figueiredo, I. Ledezma-Yanez, M. T. M. Koper, *ACS Catal.* **2016**, *6*, 2382–2392.
- [100] A. A. Peterson, F. Abild-Pedersen, F. Studt, J. Rossmeisl, J. K. Nørskov, *Energy Environ. Sci.* **2010**, *3*, 1311–1315.
- [101] N. J. Firet, W. A. Smith, *ACS Catal.* **2017**, *7*, 606–612.
- [102] J. E. Pander, III, M. F. Baruch, A. B. Bocarsly, *ACS Catal.* **2016**, *6*, 7824–7833.
- [103] C. M. Gunathunge, X. Li, J. Li, R. P. Hicks, V. J. Ovalle, M. M. Waegle, *J. Phys. Chem. C* **2017**, *121*, 12337–12344.
- [104] A. Eilert, F. S. Roberts, D. Friebel, A. Nilsson, *J. Phys. Chem. Lett.* **2016**, *7*, 1466–1470.
- [105] F. Calle-Vallejo, M. T. M. Koper, *Electrochim. Acta* **2012**, *84*, 3–11.
- [106] T. Jahnke, G. Futter, A. Latz, T. Malkow, G. Papakonstantinou, G. Tsotridis, P. Schott, M. Gérard, M. Quinaud, M. Quiroga, A. Franco, K. Malek, F. Calle-Vallejo, R. F. de Moraes, T. Kerber, P. Sautet, D. Loffreda, S. Strahl, M. Serra, P. Polverino, C. Pianese, M. Mayur, W. Bessler, C. Kompis, *J. Power Sources* **2016**, *304*, 207–233.
- [107] J. K. Nørskov, J. Rossmeisl, A. Logadottir, L. Lindqvist, J. R. Kitchin, T. Bligaard, H. Jónsson, *J. Phys. Chem. B* **2004**, *108*, 17886–17892.
- [108] A. A. Peterson, J. K. Nørskov, *J. Phys. Chem. Lett.* **2012**, *3*, 251–258.
- [109] M. T. M. Koper, *Phys. Chem. Chem. Phys.* **2013**, *15*, 1399–1407.
- [110] M. T. M. Koper, *J. Solid State Electrochem.* **2016**, *20*, 895–899.
- [111] R. Casasnovas, J. Ortega-Castro, J. Frau, J. Donoso, F. Muñoz, *Int. J. Quantum Chem.* **2014**, *114*, 1350–1363.

Chapter 2. Advances and Challenges in the Electrocatalytic conversion of Carbon Dioxide to Fuels

- [112] F. Abild-Pedersen, J. Greeley, F. Studt, J. Rossmeisl, T. R. Munter, P. Moses, E. Skúlason, T. Bligaard, J. K. Nørskov, *Phys. Rev. Lett.* **2007**, *99*, 016105.
- [113] F. Calle-Vallejo, J. I. Martínez, J. M. García-Lastra, J. Rossmeisl, M. T. M. Koper, *Phys. Rev. Lett.* **2012**, *108*, 116103.
- [114] M. M. Montemore, J. W. Medlin, *Catal. Sci. Technol.* **2014**, *4*, 3748–3761.
- [115] F. Calle-Vallejo, D. Loffreda, M. T. M. Koper, P. Sautet, *Nat. Chem.* **2015**, *7*, 403–410.
- [116] F. Calle-Vallejo, A. Krabbe, J. M. García-Lastra, *Chem. Sci.* **2017**, *8*, 124–130.
- [117] H. Shin, Y. Ha, H. Kim, *J. Phys. Chem. Lett.* **2016**, *7*, 4124–4129.
- [118] H. A. Hansen, J. B. Varley, A. A. Peterson, J. K. Nørskov, *J. Phys. Chem. Lett.* **2013**, *4*, 388–392.
- [119] Y. Li, Q. Sun, *Adv. Energy Mater.* **2016**, *6*, 1600463.
- [120] M.-J. Cheng, Y. Kwon, M. Head-Gordon, A. T. Bell, *J. Phys. Chem. C* **2015**, *119*, 21345–21352.
- [121] W. J. Durand, A. A. Peterson, F. Studt, F. Abild-Pedersen, J. K. Nørskov, *Surf. Sci.* **2011**, *605*, 1354–1359.
- [122] Z. Zhao, Z. Chen, X. Zhang, G. Lu, *J. Phys. Chem. C* **2016**, *120*, 28125–28130.
- [123] C. Shi, K. Chan, J. S. Yoo, J. K. Nørskov, *Org. Process Res. Dev.* **2016**, *20*, 1424–1430.
- [124] J. Hussain, H. Jónsson, E. Skúlason, *Faraday Discuss.* **2016**, *195*, 619–636.
- [125] H. Xiao, T. Cheng, W. A. Goddard III, *J. Am. Chem. Soc.* **2017**, *139*, 130–136.
- [126] Z. P. Jovanov, H. A. Hansen, A. S. Varela, P. Malacrida, A. A. Peterson, J. K. Nørskov, I. E. L. Stephens, I. Chorkendorff, *J. Catal.* **2016**, *343*, 215–231.